



Indoor replication of outdoor climbing routes: fidelity analysis of digital manufacturing workflow

Antonio Bacciaglia¹ · Francesco Falcetelli¹ · Raffaella Di Sante¹ · Alfredo Liverani¹ · Alessandro Ceruti¹

Received: 15 June 2023 / Accepted: 30 October 2023
© The Author(s) 2023

Abstract

This study aims to evaluate the advantages and criticalities of applying additive manufacturing to produce climbing holds replicating real rocky surfaces. A sample of a rocky surface has been reproduced with a budget-friendly 3D scanner exploiting structured light and made in additive manufacturing. The methodology is designed to build a high-fidelity replica of the rocky surface using only minor geometry modifications to convert a 2D triangulated surface into a 3D watertight model optimised for additive manufacturing. In addition, the research uses a novel design and uncertainty estimation approach. The proposed methodology proved capable of replicating a rocky sample with sub-millimetre accuracy, which is more realistic than conventional screw-on plastic holds currently used in climbing gyms. The advantages can be addressed in terms of customisation, manufacturing cost and time reduction that could lead to real outdoor climbing experiences in indoor environments by coupling additive manufacturing techniques and reverse engineering (RE). However, operating the scanner in a rocky environment and the considerable size of the climbing routes suggest that further research is needed to extend the proposed methodology to real case studies. Further analysis should focus on selecting the best material and additive manufacturing technology to produce structural components for climbing environments.

Keywords Additive manufacturing · Reverse engineering · 3D scanning · Fused deposition modelling · Uncertainty quantification · Climbing holds

1 Introduction

Opportunities for additive manufacturing (AM) have been expanding rapidly in recent decades. AM is considered a group of technologies that enable the rapid manufacture of parts from 3D digital models by layering on new material [1, 2]. AM is, therefore, developing into an effective alternative to conventional techniques. Indeed, AM has many

benefits in literature, and its applications in aerospace [3], automotive [4] and biomedical engineering [5] are growing. The advantages of designs based on AM include a shorter design-to-manufacturing time, customisation, the capacity to manufacture complicated shapes in one piece and the ability to mimic lightweight, bio-inspired structures [6]. Furthermore, due to the high degree of personalisation offered, AM can also be leveraged to realise dedicated solutions to embed Optical Fibre Sensors (OFS) into 3D printed structures for Structural Health Monitoring (SHM) applications [7].

However, AM can also be utilised as the primary production method in specific markets, such as jewellery, clothes and sporting goods. In the latter case, sport is a field that can significantly gain from the opportunities offered by AM because it enables product customisation that precisely matches the individual anatomy and performance needs of individual athletes, potentially improving comfort, performance and injury prevention [8]. A study published in the scientific literature gathered vital data on the most popular sports in various parts of the world, emphasising those

✉ Francesco Falcetelli
francesco.falcetelli@unibo.it

Antonio Bacciaglia
antonio.bacciaglia2@unibo.it

Raffaella Di Sante
raffaella.disante@unibo.it

Alfredo Liverani
alfredo.liverani@unibo.it

Alessandro Ceruti
alessandro.ceruti@unibo.it

¹ Department of Industrial Engineering (DIN), University of Bologna, Bologna, Italy

involving AM-related items [9]. These items have been broken down into three groups:

- Items that are necessary for the sport being played (such as balls, bicycles and shoes);
- Items that enhance comfort (such as soles);
- Items that protect the participant (such as helmets and shin guards).

One of the key findings from this study is that 38% of the additively manufactured sports equipment examined performs better than their conventional counterparts. The report also emphasises the current good trend of choosing AM as the primary manufacturing process. However, AM technology needs significant financing to be promoted for big batches of production; as a result, sports items made using additive production are now highly personalised and are primarily used by professional sportsmen.

Reverse engineering (RE), a group of approaches for obtaining the 3D digital geometry of a physical item, is frequently integrated with AM [10]. RE is usually used to acquire, revise or improve the topology of the target item using digital reconstruction. Helle and Lemu report the average accuracy of several RE technologies available in the market [11]. 3D scanning is the most used amongst the RE techniques due to its straightforwardness [12]. For example, Xu et al. report on scanning a historical building and 3D printing to restore stonework using the concrete deposition technique [13].

AM enables the creation of new products tailored to athletes' needs through RE techniques, nearly endless design iterations using computer-aided design (CAD) software, and the design of complex geometries that are impossible using subtractive methods. Whilst the AM-RE duo is well established in industrial engineering applications, in niche applications, such as technical sports equipment production, the scientific literature lacks fit-for-purpose examples. Amongst sports included in (Novak and Novak 2021) that use additively manufactured items, climbing is gaining popularity. This sport discipline is divided into two categories based on environmental conditions: indoor and outdoor climbing. The latter is characterised by locations not evenly distributed in the territory and sometimes challenging to reach. Moreover, the weather conditions to which they are exposed restrict their use.

However, with the technological evolution of AM and RE, it could be possible to reproduce a rocky outdoor route, combining these two technologies and installing the replicated model in indoor climbing gyms. In particular, a rocky surface can be acquired through RE approaches and manufactured with AM. The possibility of living the same sensorimotor experience, such as in outdoor rock climbing, but in a safe, regulated environment, such as a

climbing gym, can be achieved. Indeed, artificial climbing routes are available in indoor gyms, although they are not as realistic as the existing rock climbs outside.

AM for climbing has already been partially discussed in the literature. In particular, a study was conducted to replicate, through photogrammetry [14], the more challenging section of an outdoor route in a climbing gym using traditional holds [15]. The authors converted the regions used by the climber on the actual rocky route into climbing holds, much like those found in indoor climbing gyms. Thus, only the position of the holds used by the climber is reproduced. In the Whiting research, AM has been used to create a mock-up male model in Acrylonitrile Butadiene Styrene (ABS) material to create the actual mould in liquid silicone rubber.

On the other hand, Jiang et al. report on the 3D scanning and 3D printing of rock surfaces for geological studies [16]. Also in this case, 3D printing is used to manufacture the mould rather than the final product. Thus, the AM potentials of customisation and design flexibility are not extensively used in both cases [15, 16].

Another potential limitation of Whiting's research is the choice of the RE technique. Indeed, 3D scanning can gather millions of points briefly, whereas photogrammetry requires a significant number of photos to gather a dense cloud of points compared to 3D scanning [12]. In addition, it takes a very long time to acquire and digitally process the enormous number of pictures needed to create a 3D model. 3D scanning uses direct measurement techniques, such as lasers or structured light, to capture geometric data; conversely, photogrammetry reconstructs 3D data by analysing multiple 2D images taken from different viewpoints, which can introduce some errors. Last but not least, the resolution of the images used in photogrammetry strongly influences the quality of the findings; a high camera level is needed to produce a 3D model of acceptable quality.

On the one hand, the accuracy of 3D scanners can vary significantly based on the type of scanner and its specifications. High-end 3D scanners can achieve sub-millimetre or even sub-micron accuracy using laser or structured light technology. These scanners are often used in industrial metrology and engineering applications where precise measurements are required [17]. Lower cost or handheld scanners may have slightly lower accuracy but are still suitable for many applications [18]. On the other hand, the accuracy of photogrammetry can vary depending on several factors. The number and quality of images captured, camera specifications, lens quality and camera calibration accuracy all play a role. In optimal conditions, photogrammetry can achieve accuracy in the range of a few millimetres to a few centimetres [19]. However, it is important to note that photogrammetry accuracy is generally lower than in high-end 3D scanners [20].

Thus, to the authors' knowledge, applying 3D scanning, coupled with AM, to reproduce climbing holds is a never-explored application and example of fit-for-purpose combined use of AM and RE. Indeed, nowadays, climbing holds are manufactured using machined moulds where a polyurethane mixture is poured into it; after pouring, the climbing hold is left in the mould to cure, allowing for polyurethane solidification and hardening. As the last step, the hold is de-moulded and finished by sanding or buffing to smooth any rough edges and a quartz sand texture is added to enhance grip [21].

Therefore, this research aims to provide a simple, repeatable process that can faithfully recreate an entire or a section of a climbing route for indoor gyms. In contrast to [15], where a casting method was employed to create a rock wall replica, the current research proposes a feasibility study to determine whether using AM technology in climbing is practicable. This research focuses on the techniques and methods utilised for 3D scanning and AM of a rock replica to reproduce a rock face, particularly emphasising the uncertainty quantification of an AM machine and a 3D scanner. Indeed, to ensure a satisfying climbing experience, it is important to capture the geometrical details at both macro and micro scales. The importance of reproducing accurately the geometrical details at a macroscopic level is obvious.

On the other hand, the smallest geometrical details provide a certain feeling in the holding gesture and ensure the climber's proper grip. Therefore, estimating the process accuracy and the associated uncertainty is crucial. In this regard, it is important that both the RE and AM processes have comparable levels of accuracy.

Moreover, such uncertainty quantification methodology can also be extended to other fields where high replication accuracy is required. For example, in the medical field, reproducing organs for models or implant replication needs accurate details [22, 23]. Nevertheless, there are some fields of application where this concept does not strictly apply, such as civil engineering [13]. Usually, the reproduction fidelity is estimated by comparing the 3D printed model and the benchmark scanned model [19]. For example, Jiang et al. include an error analysis of natural rock joints comparing the 2D profiles at a given section of the original model, the 3D printed PLA model and the casted object [16]. However, the authors provide a qualitative estimate of the accuracy through a visual comparison rather than a quantitative and reproducible analysis.

In this article, the proposed methodology offers the possibility to decouple the uncertainty contributions of the AM technology and the RE approach, even in the presence of free-form shapes, thus without a reference CAD model. This is a unique feature since the standard practise focuses only on RE or AM accuracy estimations [11].

Such a study can be considered the first step toward manufacturing a climbing route replica for indoor installation that resembles a real one, enabling the same sensorimotor experience in an indoor gym.

The article is structured as follows. First, Sect. 2 describes the approach used to obtain the 3D-printed replica of a rocky surface. Then, Sect. 3 details the uncertainty quantification of the tools used to replicate the climbing holds and discusses the results obtained to validate the innovative methodology. In the end, Sect. 4 summarises the contribution, listing possible developments of the proposed approach.

2 Methodology

This research aims to establish a strategy that might be used to replicate a rocky surface using Additive Manufacturing, such as for indoor climbing. RE is used to acquire the morphology of the original rock to construct a replica, with a particular emphasis on the 3D scanning method based on the emission of white light. This technology enables the generation of a digital model that perfectly replicates the real component by capturing all the details and characteristics of the object.

AM technology, also called Rapid Prototyping (RP), might be used to manufacture an exact rock replica of the initial object.

The combined use of RE and AM, usually called digital manufacturing, has been explored since the emergence of AM, with a particular emphasis on mass customisation or custom-fit designs [24]. Replicating real-world things has become an important application of this relationship, along with the possibility of producing spare parts when CAD data or original tooling are unavailable [25]. A replica resembles the original item's geometry and appearance [19].

The generation of appropriate 3D models links RE and AM: whereas the former tries to create a digital description of a target object, the latter aims to fabricate shapes as specified by a 3D digital model (Fig. 1). In other words, digital fabrication, which includes AM, can be considered the inverse digitalisation process [26].

The RP approach makes it possible to produce accurate replicas compared to other manufacturing techniques without being limited by geometrical constraints. However, for the reproduction process to be supported, high-resolution 3D models are necessary. The following paragraph will describe how digital models can be gathered using image-based passive or range-based active sensors.

2.1 Reverse engineering techniques

The RE techniques are commonly used for the repair of a product, the production of spare parts or for making

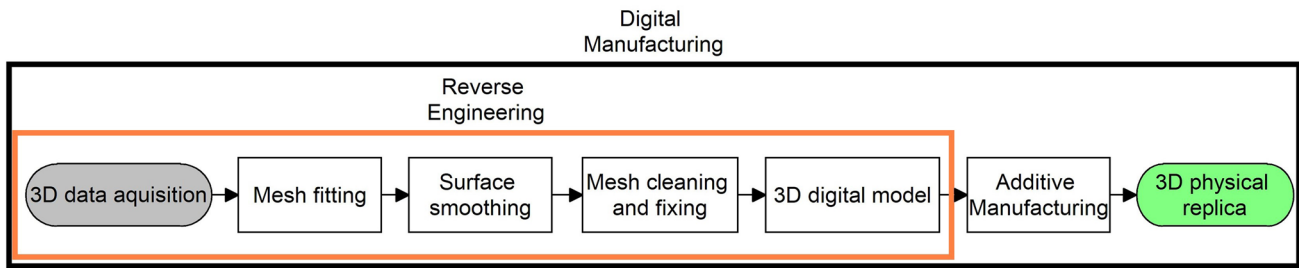


Fig. 1 General digital manufacturing workflow

modifications and improvements to an existing product. All RE techniques are based on creating a 3D point cloud to compose the digital 3D model.

The RE techniques can be divided into two main categories: the touching and optical methods. Contact methods work by direct contact between objects and instruments, such as Coordinate Measurement Machines (CMMs). Thus, no surface treatments are required to make the object's surface non-reflective; however, touching methods cannot analyse materials deformable under the contact pressure of the instrument. Optical methods are divided into active and passive approaches. In active optical methods, a light source projects the light on the object's external surface, which is reflected and captured by a sensor. The signals acquired by this sensor are then processed to obtain the 3D model (e.g. 3D scanner). Passive optical methods (i.e. photogrammetry) exploit ambient light. Images are captured from different points of view, and then the complete shape of the object is reconstructed from these [27].

Amongst active optical systems, 3D scanners are the most often used tools for mechanical engineering applications [28]. 3D scanner devices enable the acquisition of point clouds with millions of points, regardless of the object's texture, to be detected. They also allow rapid acquisition at a reduced cost. However, even though they can acquire high-resolution point clouds, they are less expensive than contact-based technologies, but they are typically less accurate and more prone to errors.

Laser, white, or other structured light sources are the basis of 3D scanners. The scanner's sensors identify the reflection of the source light after the object has received it. In particular, most surface scanning techniques leverage the principle of image triangulation of the light reflection. The x , y and z coordinates of a cloud of points are evaluated according to the known angle and distance between the light sources [29]. More and more x , y and z coordinates of sampling points are acquired as this recording is done progressively and from various angles, leading to a geometric representation of the target object.

3D scanning is widely used in entertainment, such as creating films and computer video games and conserving and exhibiting archaeological reliquaries [17].

2.2 Digital reproduction of a rocky surface

To obtain a physical replica of a rocky surface, the methodology described in this research uses the low-budget Cr-Scan 01 by Crealty [30], available from the University laboratories. To the best of the authors' knowledge, no uncertainty investigation is present in the literature for the specific model used in this research, whose characteristics are summarised in Table 1. Thus, the following section will describe a reproducible approach to estimate the replication error using a benchmark 3D model.

First, once the rocky surface under investigation has been selected, the 3D scanner is placed on its pod at a distance of 0.6 m in a dark environment. This way, the brightness of the structured light can be decreased, and the scanning procedure can be carried out easily (Fig. 2). As a first attempt, a simplified rocky surface belonging to a domestic building has been selected for this research. The wall will simulate the rocky nature of climbing routes without the logistical challenges associated with testing in an outdoor environment, such as the need for a power supply. Furthermore, the approach and case study used in this research are intentionally simplified because they

Table 1 Cr-Scan 01 characteristics by Crealty [30]

| Parameter | Value |
|---------------------------|--------------|
| Flame rate | 10 fps |
| Single frame scan range | 536 * 378 mm |
| Spatial resolution | 0.5 mm |
| Scanning distance | 400–900 mm |
| Scanning range (handheld) | 0.3–2 m |
| Scanning range (turnable) | 0.3–0.5 m |
| Output format | Obj/stl |
| Data interface | USB 3.0 |
| Operating temperature | 0–40 °C |



Fig. 2 Experimental setup to scan a sample of a rocky surface

have never been used before, and this is an initial attempt to test the procedure. The obtained surface mesh is then post-processed by the proprietary software CRStudio, and the final 2D triangulated surface mesh can be exported as a Standard Triangle Language (STL) file. Then the designer is asked to manipulate the digital model and convert the bi-dimensional surface into a manufacturable 3D model through easy and reproducible steps in a CAD software package through geometrical operations (i.e. surface offset, Boolean operations, etc.). Figure 3 represents a visual flowchart highlighting the main steps to convert a 2D rocky surface digital model into a manufacturable 3D one.

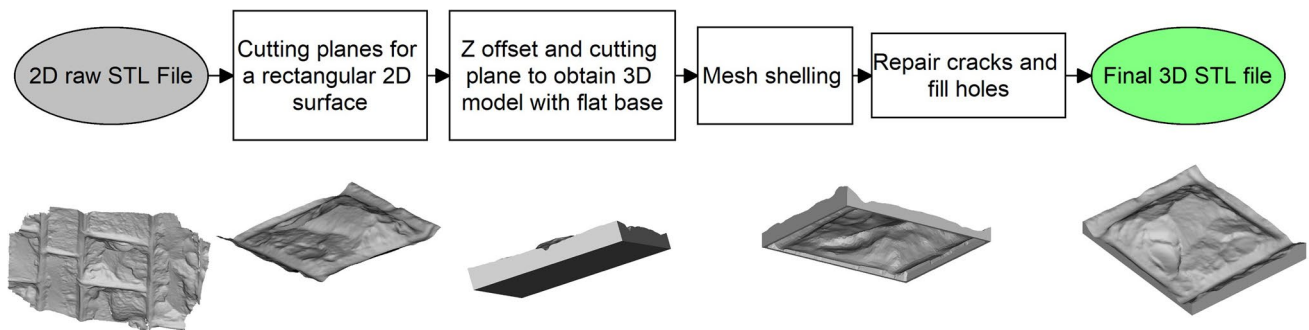


Fig. 3 CAD methodology to convert a 2D surface STL file into a watertight 3D STL model

Next, using a slicing software, the STL model is converted into a.gcode file for manufacturing purposes. This phase is required to translate a geometrical representation into a language that can be understood by automated machines (i.e. AM machines) based on a series of tasks that need to be completed. The.gcode describes the path and the machine’s necessary settings (such as how rapidly it should travel, where it should move, and several others). Finally, the.gcode file can be automatically compiled, knowing the manufacturing settings; the parameters used for this specific research are collected in Table 2.

As the last step, the generated.gcode is uploaded into an FDM machine and the rocky surface sample is manufactured in PLA (PolyLactic Acid) material for prototyping and non-structural purposes (Fig. 4). Qidi X-max is the FDM machine used to manufacture all the models of this research.

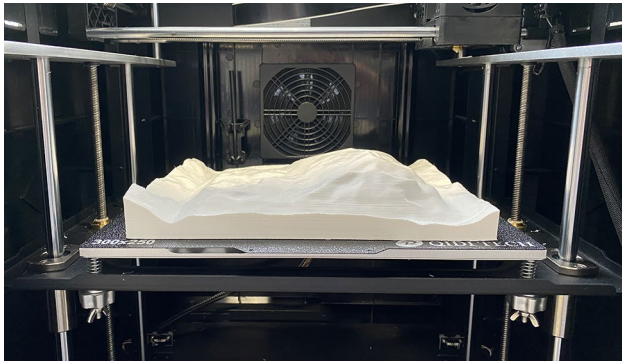
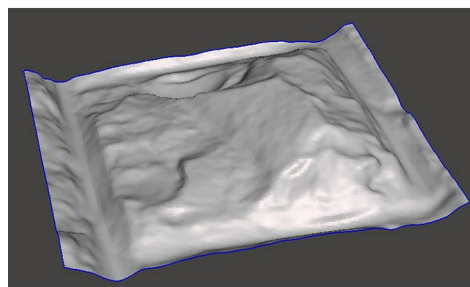
A 210 × 250 × 50 mm sample of the selected rocky surface is obtained through the FDM process. Figure 5 visually compares the 2D raw surface extracted by the 3D scanner and the manufactured object.

The choice of raw material to manufacture climbing holds and the entire replica of a climbing route is crucial: the typical material portfolio of AM technologies is particularly broad. Focussing on the FDM technique being the most common and cheaper, there are new exotic and professional materials for structural applications, such as Nylon up to reinforced polymers like Acrylonitrile Butadiene Styrene (ABS), PolyEther Ether Ketone (PEEK) and PolyPropylene (PP) with carbon or glass fibres.

As a first attempt, PLA material, which is the most user-friendly, low-budget and reproducible raw material, has been selected for the innovative application of RE and AM in manufacturing a rocky surface. Thus, the proposed methodology should be easily tested and reproducible. In any case, the choice of the most suitable material for the final structural and operative product should be supported by numerical simulations and experimental tests to evaluate the material’s behaviour with a load scenario that simulates the athlete’s presence on the climbing route.

Table 2 Slicing printing settings used for PLA filament

| Parameter | Unit | Value |
|---------------------------------|------|-------|
| Layer height | mm | 0.2 |
| Initial layer height | mm | 0.22 |
| Line width | mm | 0.43 |
| N° of bottom and top layers | – | 3 |
| Wall line count | – | 3 |
| Infill density | % | 15 |
| Infill topology | – | Lines |
| Printing temperature | °C | 215 |
| Initial printing temperature | °C | 220 |
| Build plate temperature | °C | 65 |
| Initial build plate temperature | °C | 70 |
| Flow | % | 105 |
| Print speed | mm/s | 35 |
| Initial layer print speed | mm/s | 25 |
| Travel speed | mm/s | 100 |
| Retraction distance | mm | 4 |
| Fan speed | % | 100 |
| Regular fan speed at height | mm | 0.2 |
| Support structure | – | None |

**Fig. 4** The rocky sample is manufactured with an FDM machine**Fig. 5** Visual comparison of the 2D rocky surface obtained in CRStudio (on the left) and the additively manufactured sample (on the right)

Another crucial factor in adequately selecting raw materials is the surface finishing of the climbing wall replica. The climbing wall must guarantee a solid grip; therefore, the material used to manufacture the rocky surface must have a specific surface roughness to ensure a good level of friction between the climber's hand and the wall itself and to simulate the rock surface at its best. This evaluation can be carried out through practical tests by expert climbers, proposing various prototypes of holds made with different materials to evaluate which guarantees a higher level of grip.

Subsequently, by analysing the results obtained, the material with the highest performance can be identified. A TOPSIS (Technique for Order of Preference by Similarity to Ideal Solution) analysis could help the assessment; through some calculations and matrices, it allows for obtaining the best solution amongst the different options.

These crucial evaluations will be the subject of future research and are beyond the scope of this manuscript, which is focussed on the description of a novel fit-for-purpose application of AM and RE in the reproduction of rocky surfaces.

In the following section, the uncertainty sources related to the low-budget 3D scanner and FDM machine used in this research are analysed, leveraging an ad-hoc strategy that can be easily extended to other case studies.

3 3D scanning: uncertainty analysis

3.1 Proposed strategy

The replication process introduces uncertainty in the final hold replica (see Fig. 6). First, the scanner operation is affected by uncertainty. Second, applying *Design for Additive Manufacturing* rules implies that the geometry is modified to satisfy specific requirements. For example, the hold might need to be modified to host the bolt required for the final installation. Third, FDM printing also introduces an additional uncertainty source.

Therefore, the replication accuracy is the sum of all these different contributions. In this section, the objective

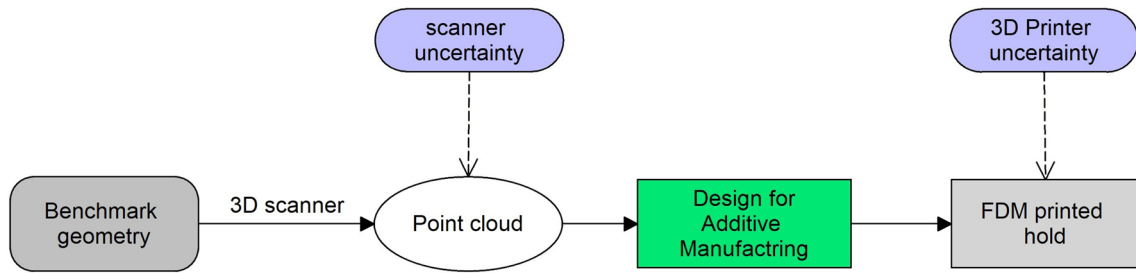


Fig. 6 Uncertainty propagation flowchart

is to assess the accuracy of the scanning and 3D printing phases. The error estimation process is shown in Fig. 7 as a flowchart.

First, a benchmark geometry containing various topological features is selected (see Fig. 8). Specifically, the selected benchmark geometry contains various holes, fillets, edges at different orientations, stair-shaped features, and possible shaded areas (where the scanning procedure is challenging). Figure 8 illustrates the abovementioned geometry providing the corresponding dimensions for different views. The reader may counter-argue about the shape of the selected benchmark object, which has all

definite geometries. On the contrary, typical rocky structures have free-form surfaces. However, those free-form topologies have random features that are hardly measurable; thus, the “ground truth” that represents the “true” or correct values that serve as a reference for evaluating the accuracy or validity of other data or models may not be available. This way, the proposed uncertainty estimation methodology may hardly apply if using free-form geometries.

Then two parts are realised with two different technologies. The first part was produced using a computer numerical control (CNC) milling machine (see Fig. 9), whereas the

Fig. 7 Error estimation flow-chart

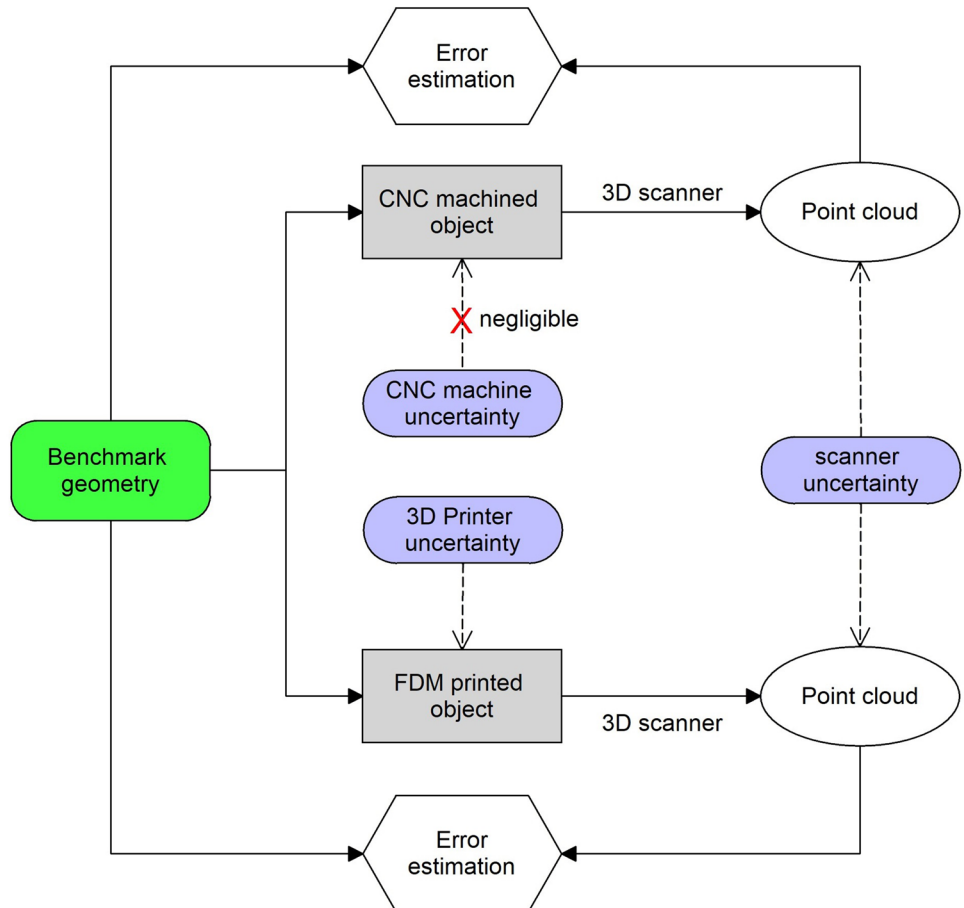


Fig. 8 CAD model of the benchmark geometry (the dimensions reported are in millimetres [mm])

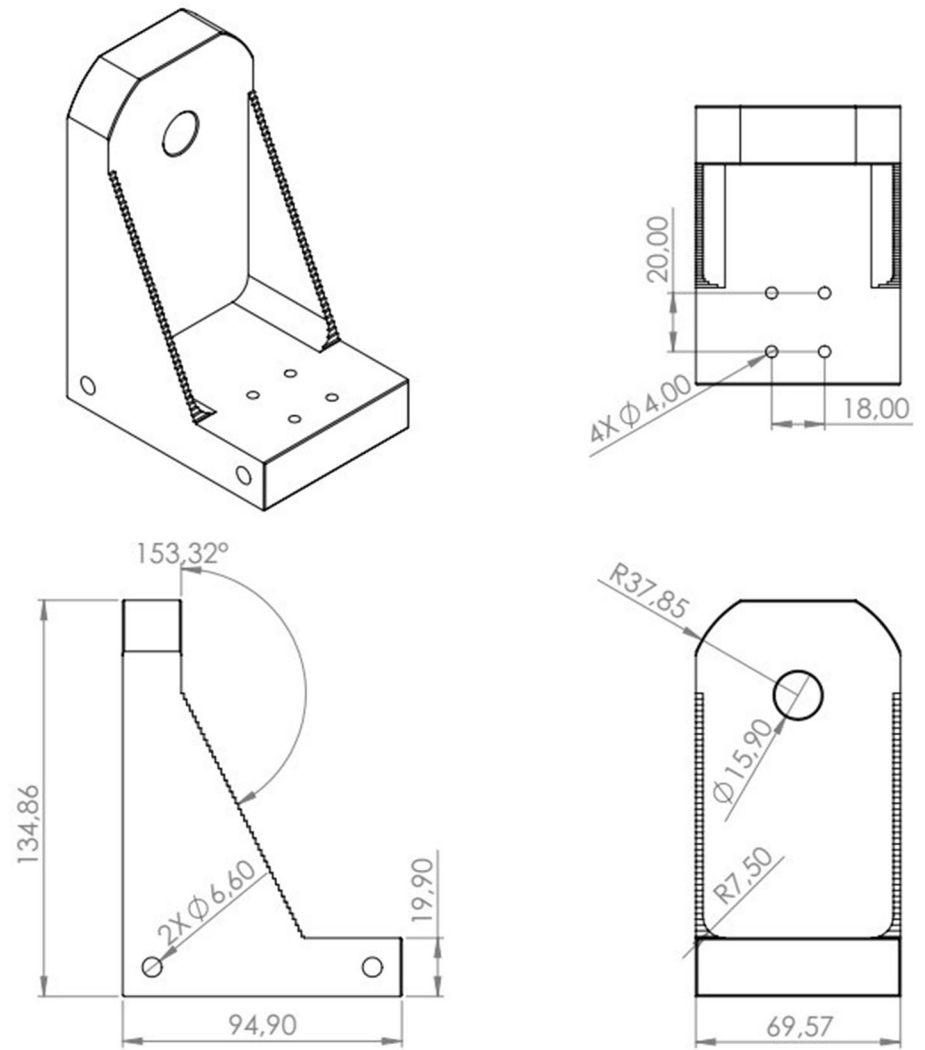


Fig. 9 CNC manufacturing of the benchmark geometry: lateral view (a) and front view (b)

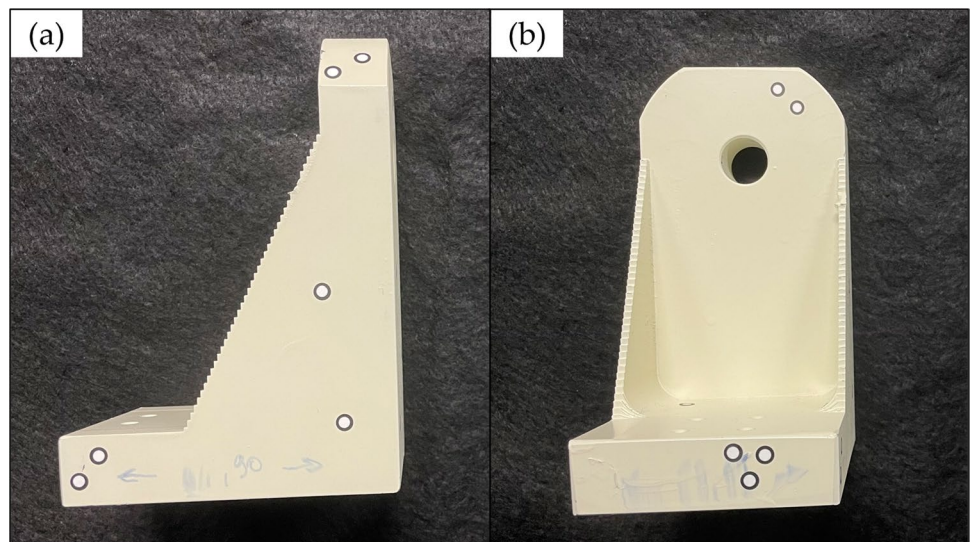
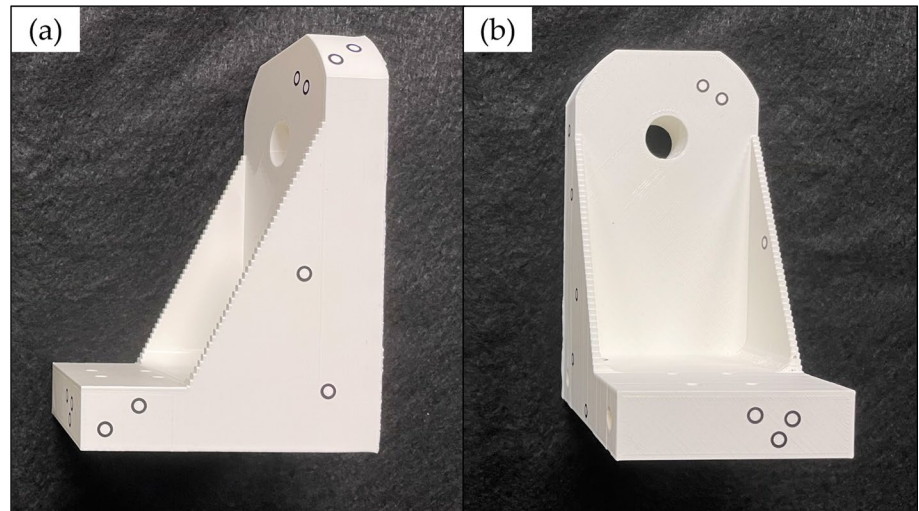


Fig. 10 FDM manufacturing of the benchmark geometry: lateral view (a) and front view (b)



second was built using the FDM Additive Manufacturing technique (see Fig. 10).

After conditioning the surfaces of both parts with white painting to reduce reflectivity [31], several point markers were employed in the scanning process to improve accuracy. The optimal configuration, identified after a trial and error procedure, was adopted for both manufactured parts (see Figs. 9 and 10).

The experimental setup used to obtain the point clouds of the two manufactured objects is shown in Fig. 11.

Finally, the point clouds are compared with the original mesh of the benchmark geometry through the open-source CloudCompare software [32], which has already been used in similar applications [19].

Previous experimental activities showed that the CNC milling machine has an accuracy of at least one order of magnitude higher than the uncertainty sources under investigation.

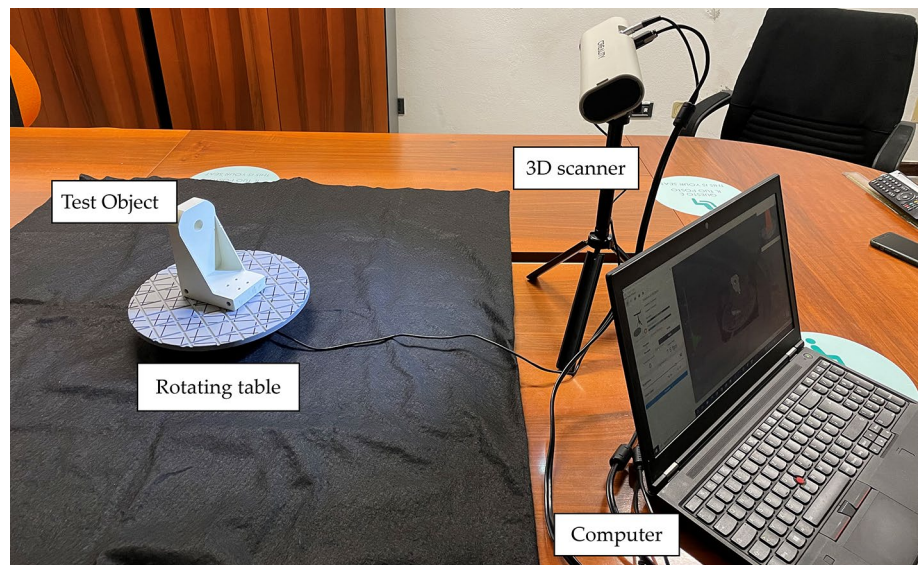
Therefore, the uncertainty estimation can be associated entirely with the scanning operation in the first case. On the other hand, in the second case, the uncertainty is made of both the printing and scanning contributions. Then the accuracy of the FDM process can be obtained by subtracting the uncertainty estimated in the two cases.

Four scanning operations were carried out for both scenarios. In each scanning, the CloudCompare software returns \bar{x} and S_x , the average distance and the standard deviation of the point pairs in the point clouds.

Then it is possible to compute the pooled mean as described by Eq. (1):

$$\langle \bar{x} \rangle = \frac{1}{M} \sum_{j=1}^M \bar{x}_j, \quad (1)$$

Fig. 11 Experimental setups with labels



where M symbolises the number of replications, corresponding with the number of scanning operations. Similarly, Eq. (2) provides the formula to compute the pooled standard deviation:

$$\langle S_x \rangle = \sqrt{\frac{1}{M} \sum_{j=1}^M S_{x_j}^2} \tag{2}$$

3.2 Uncertainty analysis: results and discussion

Figure 12 reports an illustrative example of the dimensional analysis carried out within CloudCompare. In the colour bar on the right-hand side, units are in millimetres, and the acronym C2M stands for Clod-to-Mesh distance taken with its sign [32]. Positive values (red colour in Fig. 12) identify regions where the point cloud estimated by scanning the object is outside the region enclosed by the benchmark point cloud. Analogously, negative values (blue colour in Fig. 12) symbolise areas where the benchmark point cloud encloses the estimated point cloud. From a qualitative perspective, it is already possible to notice how critical are the fillet regions.

As anticipated in the previous section, the analysis compared the benchmark point clouds with the point clouds obtained by scanning the CNC-machined object and the

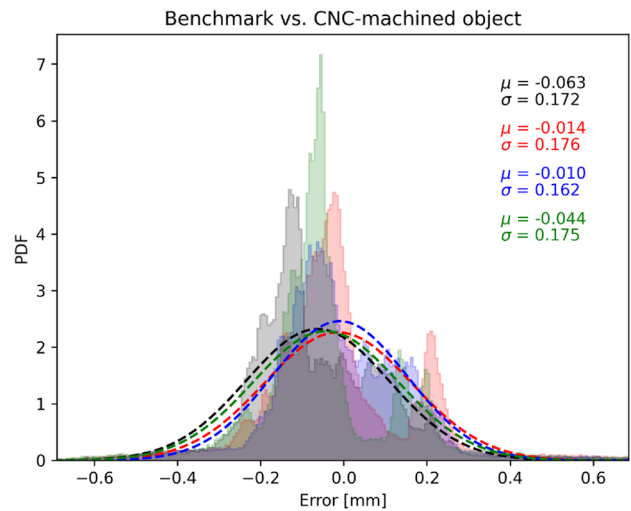
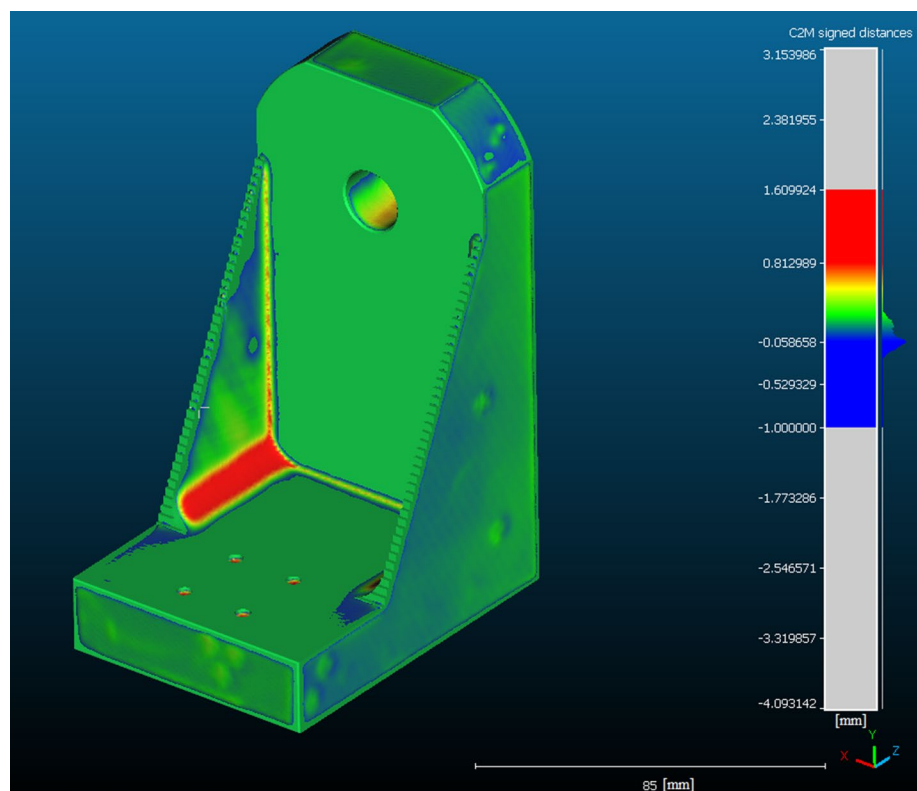


Fig. 13 Scanner error distribution obtained as the point clouds differences between the benchmark and the CNC object

FDM printed object. The results of this analysis are summarised in Figs. 13 and 14. These two figures show the error distributions for the four scanning operations, reporting the mean and the standard deviation for each scan. The dashed lines represent normal probability distributions using the computed values as mean and standard deviations. Data are

Fig. 12 Example of point cloud analysis with CloudCompare (the dimensions reported are in millimetres)



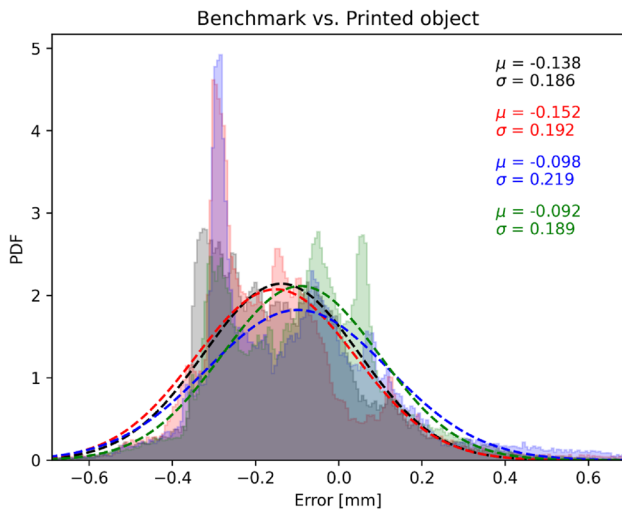


Fig. 14 Scanner error distribution obtained as the point clouds differences between the benchmark and the printed object

Table 3 Uncertainty analysis results of the benchmark geometry

| | Case 1 | Case 2 | Δ |
|--------------------------------|--------|--------|----------|
| Number of measurements | 4 | 4 | – |
| Average point cloud size | 96,094 | 98,082 | – |
| Pooled mean (mm) | –0.03 | –0.12 | –0.09 |
| Pooled standard deviation (mm) | 0.17 | 0.20 | 0.03 |

not necessarily normally distributed, and the Gaussian distributions serve only as auxiliary visualisation tools.

The results are summarised in Table 3, where Case 1 denotes the benchmark vs CNC-machined object, whereas Case 2 indicates the benchmark versus FDM printed object. In addition, Table 3 reports the number of measurements (four in both cases), the average number of points in the respective point clouds and the pooled mean and standard deviation (see Eqs. 1 and 2).

The two clouds of points are of comparable sizes, which is expected since the geometry is the same in both cases. The main difference is in the pooled mean values, representing the average shrinkage or enlargement of the point cloud compared to the benchmark geometry. In Case 1, the pooled mean is close to zero, reflecting that the scanning operation does not alter the average object size in the absence of manufacturing inaccuracies (CNC machine uncertainty source is negligible). On the other hand, Case 2 shows a pooled mean value of –0.12 mm. Computing the difference between the two cases, one obtains the Δ value given in the last column of Table 3, which represents the net shrinkage effect only due to the FDM printing process. The Δ which is related to the pooled mean is equal to –0.09 mm. The pooled standard deviation can be interpreted as a metric for scanner

accuracy. The results show comparable values in both cases, 0.17 and 0.20 mm, respectively. The slightly higher value of Case 2 can be attributed to the higher uncertainty associated with the FDM manufacturing process compared to the CNC milling technique.

This analysis provided a tool to decouple the scanning and manufacturing uncertainty sources. Similar results are expected for the rocky surface under investigation in this study. It was impossible to perform the same procedure directly on the rocky surface because the benchmark geometry would not be available. However, the proposed strategy provides the expected accuracy for geometry reconstruction.

4 Conclusion and future developments

Through the use of RE techniques, new products can be created that are specifically suited to the requirements of athletes because of the high design flexibility provided by Additive Manufacturing.

In this study, a novel method for reproducing a rocky outdoor route is investigated, with the possibility—in the near future—of installing the replicated model in indoor climbing gyms. This approach might allow a similar sensorimotor experience—like outdoor rock climbing—in a controlled environment, like a climbing gym.

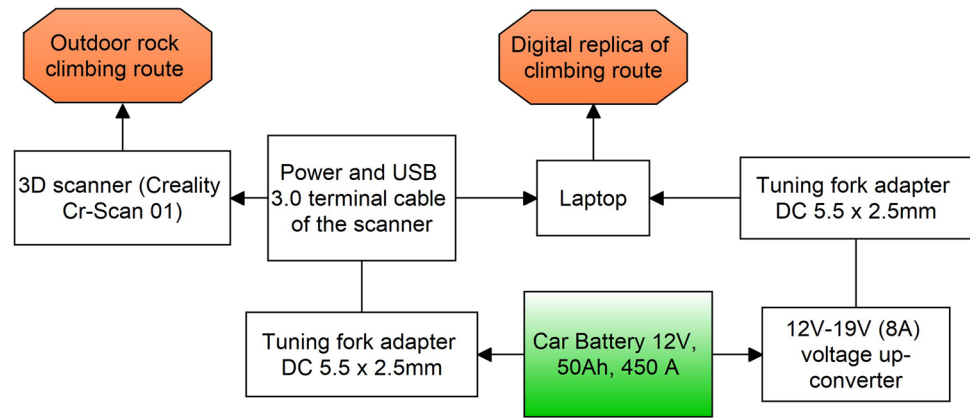
A sample of a rocky surface has been successfully replicated using a budget-friendly 3D scanner with structured light, a RE technique that has never been used in the scientific literature previously for this specific application. Such a choice is coherent with the needs of a niche sport application such as climbing, where it is reasonable to assume that low budget might be available for the RE equipment.

The proposed methodology is designed to produce a high-fidelity replica of the rocky surface without the user needing any special prior knowledge. However, only minor geometry modification, described step-by-step, is necessary to convert a 2D triangulated surface into a 3D watertight model optimised for additive manufacturing. Moreover, the manuscript includes a specific and deeply described methodology to quantify the uncertainty sources of the 3D scanner and the FDM machine. The analysis is fundamental to estimating the replication process’s accuracy level at both macro and micro scales.

The results showed that the value of the pooled mean, which represents the uncertainty source associated with the FDM machine, is $\Delta = -0.09$ mm. The scanner accuracy is represented by the pooled standard deviation of Case 1 and is estimated to be 0.17 mm; indeed, the CNC manufacturing process uncertainty can be neglected.

The uncertainty analysis revealed that the digital manufacturing workflow has a submillimeter accuracy and, therefore, is adequate for replicating climbing routes,

Fig. 15 Possible setup to supply power to the 3D scanner in outdoor conditions



characterised by topological features whose dimensions are usually of a higher order of magnitudes. Such a level of accuracy is needed to reproduce the main surface features of rocky cliffs even for small holds of roughly 50–100 mm in diameter, which is common amongst the premier climbing hold retailers [21], or to increase the sensorimotor experience of large hold panels, which is relevant also for recreational purposes.

The proposed uncertainty quantification methodology proved effective for this specific application, but in principle, it can also be extended to different applications with an equivalent production workflow. The scanning and realisation of an entire outdoor climbing wall are not trivial. First, the 3D scanner should be portable and compatible with a handheld configuration. This requirement is often difficult to achieve when high levels of accuracy are required [16]. Moreover, the scanner power supply source is a critical issue with 3D scanning in an outdoor environment. Typically, the scanner is connected to the mains in indoor conditions via the traditional power supply; such conditions should be replicated externally. Therefore, the authors propose a simple layout designed to solve the issue above, as shown in Fig. 15.

Moreover, since the rocky surface is of considerable size, a simple scan performed by the operator at the foot of the wall is insufficient due to a limited single-frame scan range. Therefore, some solutions to overcome this problem could be:

- Abseil down the wall using a special harness and ropes whilst the operator scans the wall holding the scanner with one hand;
- Place the scanner on a drone remotely controlled by the operator to scan the entire wall.

The first solution is undoubtedly cheaper but less precise, whilst the second offers higher stability. Once the complete scan of the wall has been completed, it is possible to proceed with the manufacturing process with AM machines. However, this stage, in the same way, is affected by the large

dimensions of the object to be manufactured. For this reason, it is impossible to get the whole wall using a single large model only, but a practical solution could be to split the entire climbing wall into several small rectangular tiles that are manufactured individually and subsequently assembled to form the complete route to be installed in an indoor gym.

However, these activities are evidently beyond the scope of this preliminary research, whose primary outcome is to propose a step-by-step methodology to estimate the digital manufacturing workflow accuracy, distinguishing between the RE and AM levels of uncertainty. Compared to the discussed literature, the conceptualisation of a reproducible methodology aims to provide a significant contribution to the field.

Applying the methodology in relevant environments, such as actual cliff faces, is the object of ongoing research projects at our laboratories. In the near future, the authors would like to apply this methodology to obtain a ready-to-market product.

The authors believe that all the abovementioned challenges deserve further investigation and will be the subject of future research.

Funding Open access funding provided by Alma Mater Studiorum - Università di Bologna within the CRUI-CARE Agreement.

Data availability Neither data, material nor code is available due to future work in the same project.

Declarations

Conflict of interest On behalf of all authors, the corresponding author states that there is no conflict of interest.

Open Access This article is licensed under a Creative Commons Attribution 4.0 International License, which permits use, sharing, adaptation, distribution and reproduction in any medium or format, as long as you give appropriate credit to the original author(s) and the source, provide a link to the Creative Commons licence, and indicate if changes were made. The images or other third party material in this article are included in the article's Creative Commons licence, unless indicated otherwise in a credit line to the material. If material is not included in the article's Creative Commons licence and your intended use is not

permitted by statutory regulation or exceeds the permitted use, you will need to obtain permission directly from the copyright holder. To view a copy of this licence, visit <http://creativecommons.org/licenses/by/4.0/>.

References

- Bacciaglia A, Falchetti F, Troiani E et al (2022) Geometry reconstruction for additive manufacturing: from G-CODE to 3D CAD model. *Mater Today Proc* 75:16–22. <https://doi.org/10.1016/j.matpr.2022.09.496>
- Mawale MB, Kuthe AM, Dahake SW (2016) Additive layered manufacturing: state-of-the-art applications in product innovation. *Concurr Eng* 24:94–102. <https://doi.org/10.1177/1063293X15613111>
- Pecho P, Ažaltovič V, Kandra B, Bugaj M (2019) Introduction study of design and layout of UAVs 3D printed wings in relation to optimal lightweight and load distribution. *Transp Res Procedia* 40:861–868. <https://doi.org/10.1016/j.trpro.2019.07.121>
- Chinthavali M (2016) 3D printing technology for automotive applications. In: 2016 International Symposium on 3D Power Electronics Integration and Manufacturing (3D-PEIM). IEEE, Raleigh, NC, USA, p 1–13
- Savio G, Rosso S, Meneghello R, Concheri G (2018) Geometric modeling of cellular materials for additive manufacturing in biomedical field: a review. *Appl Bionics Biomech* 2018:1–14. <https://doi.org/10.1155/2018/1654782>
- Campbell I, Bourell D, Gibson I (2012) Additive manufacturing: rapid prototyping comes of age. *Rapid Prototyp J* 18:255–258. <https://doi.org/10.1108/13552541211231563>
- Falchetti F, Di Sante R, Troiani E (2021) Strategies for embedding optical fiber sensors in additive manufacturing structures. In: Rizzo P, Milazzo A (eds) *European workshop on structural health monitoring*. Springer, Cham, pp 362–371
- Binelli MR, van Dommelen R, Nagel Y et al (2023) Digital manufacturing of personalised footwear with embedded sensors. *Sci Rep* 13:1962. <https://doi.org/10.1038/s41598-023-29261-0>
- Novak JI, Novak AR (2021) Is additive manufacturing improving performance in Sports? A systematic review. *Proc Inst Mech Eng Part P J Sports Eng Technol* 235:163–175. <https://doi.org/10.1177/1754337120971521>
- Laroche F, Bernard A, Cotte M (2008) Advanced industrial archaeology: A new reverse-engineering process for contextualising and digitising ancient technical objects. *Virtual Phys Prototyp* 3:105–122. <https://doi.org/10.1080/17452750802045028>
- Helle RH, Lemu HG (2021) A case study on use of 3D scanning for reverse engineering and quality control. *Mater Today Proc* 45:5255–5262. <https://doi.org/10.1016/j.matpr.2021.01.828>
- Geng Z, Bidanda B (2017) Review of reverse engineering systems – current state of the art. *Virtual Phys Prototyp* 12:161–172. <https://doi.org/10.1080/17452759.2017.1302787>
- Xu J, Ding L, Love PED (2017) Digital reproduction of historical building ornamental components: from 3D scanning to 3D printing. *Autom Constr* 76:85–96. <https://doi.org/10.1016/j.autcon.2017.01.010>
- Schindler K (2015) Mathematical foundations of photogrammetry. In: Freeden W, Nashed M, Sonar T (eds) *Handbook of geomathematics*. Springer, Berlin
- Whiting E, Ouf N, Makatura L, et al. (2017) Environment-scale fabrication: replicating outdoor climbing experiences. In: *Proc. 2017 CHI conference on human factors in computing systems*. ACM, p. 1794–1804
- Jiang Q, Feng X, Gong Y et al (2016) Reverse modelling of natural rock joints using 3D scanning and 3D printing. *Comput Geotech* 73:210–220. <https://doi.org/10.1016/j.compgeo.2015.11.020>
- Drenik M, Kampel M (2008) An evaluation of low cost scanning versus industrial 3D scanning devices. In: 2008 Congress on Image and Signal Processing. IEEE, Sanya, China, p 756–760
- Dessery Y, Pallari J (2018) Measurements agreement between low-cost and high-level handheld 3D scanners to scan the knee for designing a 3D printed knee brace. *PLoS ONE* 13:e0190585. <https://doi.org/10.1371/journal.pone.0190585>
- Bonora V, Tucci G, Meucci A, Pagnini B (2021) Photogrammetry and 3D printing for marble statues replicas: critical issues and assessment. *Sustainability* 13:680. <https://doi.org/10.3390/su13020680>
- Baltsavias EP (1999) A comparison between photogrammetry and laser scanning. *ISPRS J Photogramm Remote Sens* 54:83–94. [https://doi.org/10.1016/S0924-2716\(99\)00014-3](https://doi.org/10.1016/S0924-2716(99)00014-3)
- (2023) Mimic Holds. In: Holds shaped by nature. <https://www.mimicholds.com/>. Accessed 23 Aug 2023
- Jin Z, Li Y, Yu K et al (2021) 3D printing of physical organ models: recent developments and challenges. *Adv Sci* 8:2101394. <https://doi.org/10.1002/advs.202101394>
- Okkalidis N, Marinakis G (2020) Technical note: accurate replication of soft and bone tissues with 3D printing. *Med Phys* 47:2206–2211. <https://doi.org/10.1002/mp.14100>
- Solaberrieta E, Amezua X, Garikano X et al (2021) Customization of Kayak Paddle grips by using reverse engineering, computer aided design and additive manufacturing tools. In: Roucoules L, Paredes M, Eynard B et al (eds) *Advances on mechanics, design engineering and manufacturing III*. Springer, Cham, pp 261–267
- Zhang X, Cui W, Li W, Liou F (2019) A hybrid process integrating reverse engineering, pre-repair processing, additive manufacturing, and material testing for component remanufacturing. *Materials* 12:1961. <https://doi.org/10.3390/ma12121961>
- Rossoni M, Colombo G (2019) Replicas fabrication by laser scanner and additive manufacturing: A preliminary investigation. In: *ASME International Mechanical Engineering Congress and Exposition, Proceedings (IMECE)*
- Bacciaglia A, Ceruti A, Liverani A (2020) Photogrammetry and additive manufacturing based methodology for decentralised spare part production in automotive industry. In: Ahram T, Karwowski W, Vergnano A et al (eds) *Intelligent human systems integration 2020*. Springer, Cham, pp 796–802
- Afteni C, Paunoiu V, Afteni M, Teodor V (2022) Using 3D scanning in assessing the dimensional accuracy of mechanically machined parts. *IOP Conf Ser: Mater Sci Eng* 1235:012071. <https://doi.org/10.1088/1757-899X/1235/1/012071>
- Markus B, García-Martínez D, Torres-Tamayo N et al (2019) Workflows in a virtual morphology lab: 3D scanning, measuring, and printing. *J Anthropol Sci* 96:107–134. <https://doi.org/10.4436/JASS.97003>
- Creality (2020) Cr Scan-01. <https://rb.gy/54pdum>. Accessed 13 Mar 2023
- Boehler W, Vicent M, Marbs A (2003) Investigating laser scanner accuracy. *Proc CIPA XIXth Int Symposium* 34:
- CloudCompare (2015) User manual - version 2.6.1. CloudCompare

Publisher's Note Springer Nature remains neutral with regard to jurisdictional claims in published maps and institutional affiliations.